AMERICAN SOCIETY FOR MICROBIOLOGY | mBio®

RESEARCH ARTICLE
Host-Microbe Biology

Syntrophy via Interspecies H_2 Transfer between *Christensenella* and *Methanobrevibacter* Underlies Their Global Cooccurrence in the Human Gut

Albane Ruaud,[a] Sofia Esquivel-Elizondo,[a,b] Jacobo de la Cuesta-Zuluaga,[a] Jillian L. Waters,[a] Largus T. Angenent,[b] Nicholas D. Youngblut,[a] Ruth E. Ley[a]

[a]Department of Microbiome Science, Max Planck Institute for Developmental Biology, Tübingen, Germany
[b]Center for Applied Geosciences, Eberhard-Karls-Universität Tübingen, Tübingen, Germany

Albane Ruaud and Sofia Esquivel-Elizondo contributed equally to this work. Author order was determined on the basis of substantial relative-contribution differences.

ABSTRACT Across human populations, 16S rRNA gene-based surveys of gut microbiomes have revealed that the bacterial family *Christensenellaceae* and the archaeal family *Methanobacteriaceae* cooccur and are enriched in individuals with a lean, compared to an obese, body mass index (BMI). Whether these association patterns reflect interactions between metabolic partners, as well as whether these associations play a role in the lean host phenotype with which they associate, remains to be ascertained. Here, we validated previously reported cooccurrence patterns of the two families and their association with a lean BMI with a meta-analysis of 1,821 metagenomes derived from 10 independent studies. Furthermore, we report positive associations at the genus and species levels between *Christensenella* spp. and *Methanobrevibacter smithii*, the most abundant methanogen of the human gut. By coculturing three *Christensenella* spp. with *M. smithii*, we show that *Christensenella* spp. efficiently support the metabolism of *M. smithii* via H_2 production far better than *Bacteroides thetaiotaomicron* does. *Christensenella minuta* forms flocs colonized by *M. smithii* even when H_2 is in excess. In culture with *C. minuta*, H_2 consumption by *M. smithii* shifts the metabolic output of *C. minuta*'s fermentation toward acetate rather than butyrate. Together, these results indicate that the widespread cooccurrence of these microorganisms is underpinned by both physical and metabolic interactions. Their combined metabolic activity may provide insights into their association with a lean host BMI.

IMPORTANCE The human gut microbiome is made of trillions of microbial cells, most of which are *Bacteria*, with a subset of *Archaea*. The bacterial family *Christensenellaceae* and the archaeal family *Methanobacteriaceae* are widespread in human guts. They correlate with each other and with a lean body type. Whether species of these two families interact and how they affect the body type are unanswered questions. Here, we show that species within these families correlate with each other across people. We also demonstrate that particular species of these two families grow together in dense flocs, wherein the bacteria provide hydrogen gas to the archaea, which then make methane. When the archaea are present, the ratio of bacterial products (which are nutrients for humans) is changed. These observations indicate that when these species grow together, their products have the potential to affect the physiology of their human host.

KEYWORDS human gut, methanogens, microbiome, syntrophy

Citation Ruaud A, Esquivel-Elizondo S, de la Cuesta-Zuluaga J, Waters JL, Angenent LT, Youngblut ND, Ley RE. 2020. Syntrophy via interspecies H_2 transfer between *Christensenella* and *Methanobrevibacter* underlies their global cooccurrence in the human gut. mBio 11:e03235-19. https://doi.org/10.1128/mBio.03235-19.

Editor Martin J. Blaser, Rutgers University

Address correspondence to Ruth E. Ley, rley@tuebingen.mpg.de.

This article is a direct contribution from Ruth E. Ley, a Fellow of the American Academy of Microbiology, who arranged for and secured reviews by Rob Knight, UCSD School of Medicine, and Daniel Buckley, Cornell University.

Received 10 December 2019
Accepted 12 December 2019
Published 4 February 2020

Obesity was the first human disease phenotype to be associated with an altered microbial ecology of the gut (1, 2). The link between the relative abundance in the gut of the bacterial family *Christensenellaceae* and a low host body mass index (BMI) now stands as one of the most robust associations described between the human gut microbiome and host BMI (3–15). Compared to other families of bacteria that comprise the human gut microbiome, the family *Christensenellaceae* was described relatively recently, when the type strain, *Christensenella minuta*, was reported in 2012 (16). Prior to the description of *C. minuta*, 16S rRNA sequences from this genus escaped notice in the gut microbiome, though these sequences accumulated steadily in small-subunit (SSU) rRNA gene databases. A positive association between a lean host BMI and the relative abundance in the gut of *Christensenellaceae* 16S rRNA genes was first reported in 2014 (4). The association was shown to have existed in earlier data sets (4) but was likely undetected, as this family had not yet been named. Goodrich et al. showed a causal link between the *Christensenellaceae* and host BMI in gnotobiotic mice: the addition of *C. minuta* to the gut microbiome of an obese human donor prior to transplantation reduced adiposity gains in the recipient mice compared to those of controls receiving the unsupplemented microbiome (4). The mechanism underlying this host response remains to be elucidated. One step toward this goal is a better understanding of how the members of the *Christensenellaceae* interact ecologically with other members of the gut microbiome.

Across human populations, the gut microbiota often forms patterns of cooccurrence (e.g., when these consortia exist in a subset of human subjects, they are termed enterotypes [17]). Such cooccurrences of taxa across subjects reflect shared environmental preferences, but to determine if they represent metabolic or physical interactions requires further study. The family *Christensenellaceae* consistently forms the hub of cooccurrence networks with other taxa (6, 8, 9, 18, 19). Notably, gut methanogens (specifically, of the archaeal family *Methanobacteriaceae*) are often reported as part of the *Christensenellaceae* cooccurrence consortium (4, 20–22). The most widespread and abundant of the gut methanogens, *Methanobrevibacter smithii*, produces CH_4 from H_2 and CO_2, the products of bacterial fermentation of dietary fibers. Such cross-feeding likely explains why the relative abundances of *M. smithii* and fermenting bacteria are often positively correlated (21, 23, 24). Several studies have shown that in the laboratory, *M. smithii* can grow from the H_2 provided by *Bacteroides thetaiotaomicron*, a common gut commensal bacterium (25–27). Given that the cultured representatives of the *Christensenellaceae* ferment simple sugars (16, 28) and that their genomes contain hydrogenases (29), we predicted that members of the *Christensenellaceae* produce H_2 used by *M. smithii* as a substrate in methanogenesis.

Here, we explored the association between the *Christensenellaceae* and the *Methanobacteriaceae* in two ways. First, we analyzed metagenomes for statistical associations between the two families and their subtaxa. Compared to 16S rRNA gene surveys, metagenomes often can better resolve the taxonomic assignments of sequence reads below the genus level (30). Metagenome-based studies have so far been blind to the *Christensenellaceae*, however, because their genomes have been lacking from reference databases. Here, we customized a reference database to include *Christensenellaceae* genomes, which we used in a meta-analysis of >1,800 metagenomes from 10 studies. Second, to assess for metabolic interactions between members of the *Christensenellaceae* and *Methanobacteriaceae*, we measured methane production by *M. smithii* when grown in coculture with *Christensenella* spp. Our results show that (i) the positive association between the *Christensenellaceae* and the *Methanobacteriaceae* is robust to the genus/species level across multiple studies, (ii) these taxa associate with a lean host BMI, (iii) *Christensenella* spp. support the growth of *M. smithii* by interspecies H_2 transfer far better than *B. thetaiotaomicron* does, and (iv) *M. smithii* directs the metabolic output of *C. minuta* toward less butyrate and more acetate and H_2, which is consistent with reduced energy availability to the host and consistent with the association with a low BMI.

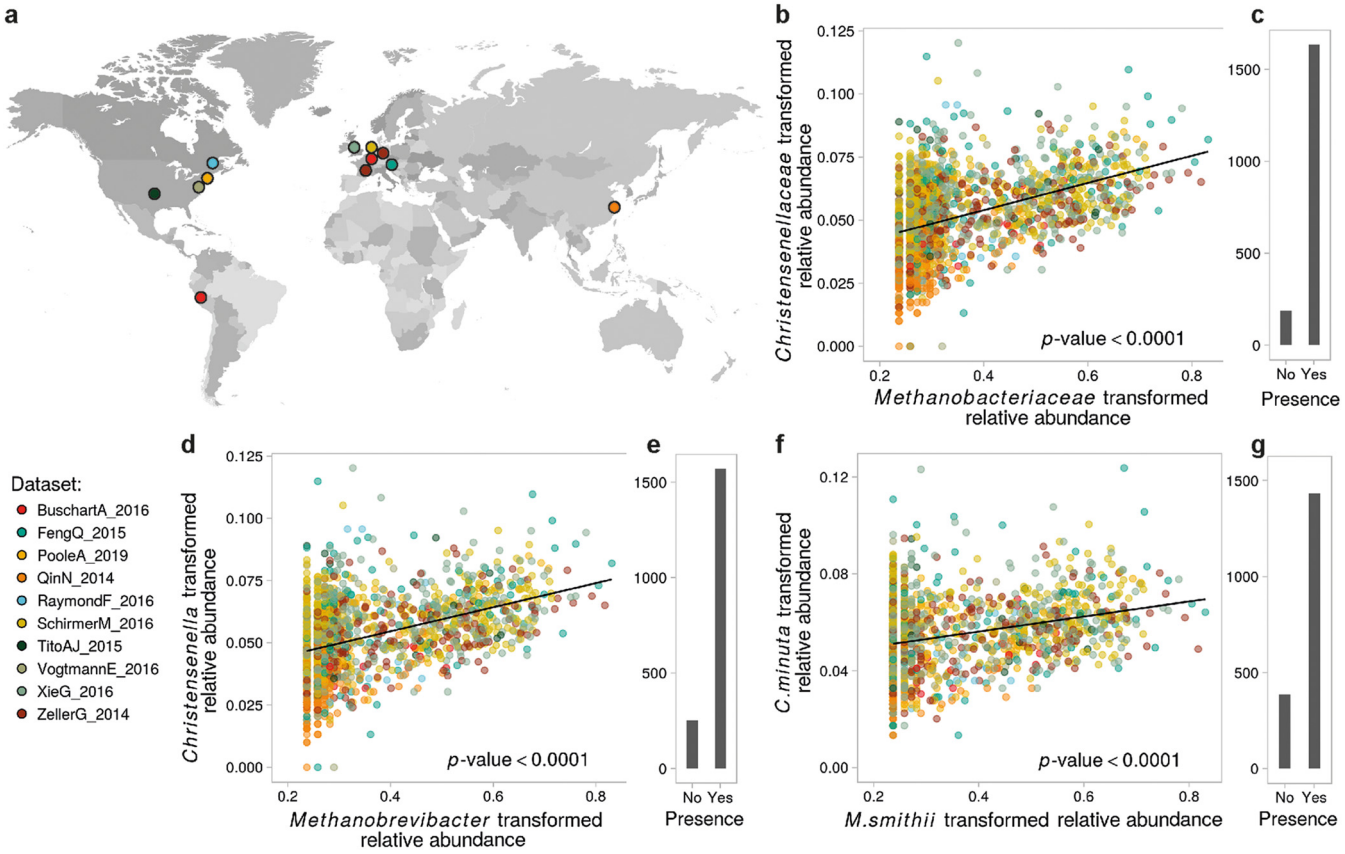

FIG 1 Abundances of the *Methanobacteriaceae* and *Christensenellaceae* families across populations. (a) Countries where the human gut metagenomes used in our meta-analysis ($n = 1,821$ samples) were recruited by 10 independent studies (summarized in Table S3); (b) association between the transformed relative abundances of *Christensenellaceae* and *Methanobacteriaceae* in samples where the a member of the *Methanobacteriaceae* was detected; (c) numbers of samples in which the *Methanobacteriaceae* were detected; (d and e and f and g) same as panels b and c at the genus and species levels, respectively. The correlation between the transformed relative abundances of both taxa at each taxonomic level was evaluated using linear mixed models to correct for covariates (ANOVA, *P* values < 0.0001).

RESULTS

***Christensenella* relative abundance is significantly correlated with leanness across populations.** Both the *Christensenellaceae* family and the genus *Christensenella* had very high prevalences, as they were present in more than 99% of the 1,821 samples; both the family and the genus have a mean abundance of 0.07% ± 0.05% (Fig. 1b and d and see Fig. S1 in the supplemental material). To correct for the influence of environmental factors on the relative abundances of members of the *Christensenellaceae* family and of the *Christensenella* genus, we first constructed null models in which we selected covariates (see Appendix 1 in Text S1) that explained a significant proportion of the variance of the transformed relative abundance of the family *Christensenellaceae* and in the same manner as that of the *Christensenella* genus. BMI and age were significantly correlated with the transformed relative abundances of members of the *Christensenellaceae* family and of the *Christensenella* genus (Cf-tra and Cg-tra, respectively, where the suffix "-tra" indicates transformed abundances) and were retained in the null models (Cf-null and Cg-null).

BMI was negatively correlated with both Cf-tra (type II analysis of variance [ANOVA], *P* value = 0.0002 and *F* value [339] = 14.46) and Cg-tra (type II ANOVA, *P* value = 0.0002 and *F* value [339] = 14.29), indicating that leaner individuals harbor higher relative abundances of *Christensenellaceae* and *Christensenella*. Age was negatively correlated with Cf-tra (type II ANOVA, *P* value = 0.01 and *F* value [1,468] = 6.56) and with Cg-tra (type II ANOVA, *P* value = 0.01 and *F* value [1,468] = 6.53), indicating that younger subjects carry greater relative abundances of *Christensenellaceae* and *Christensenella*.

However, the interaction term between BMI and age was not significantly correlated with the transformed relative abundances (type II ANOVA, P values > 0.1), indicating that their effects are additive. These results show that regardless of their BMIs, younger subjects have higher levels of *Christensenellaceae* and *Christensenella* and that the lower a subject's BMI, the more of these microbes they harbor, regardless of their age.

***Methanobrevibacter* relative abundance is significantly correlated with leanness across populations.** The *Methanobacteriaceae* family and *Methanobrevibacter* genus also had high prevalences, with 92% and 89% of people harboring them, respectively, and with mean abundances of 0.48% ± 1.55% and 0.49% ± 1.54%, respectively. As described above, we evaluated the association between the *Methanobacteriaceae* family and of the *Methanobrevibacter* genus by using models for BMI and age (models Mf-null and Mg-null). The transformed relative abundances of *Methanobacteriaceae*, Mf-tra, and of *Methanobrevibacter*, Mg-tra, were also negatively correlated with BMI (type II ANOVA, respective P values = 0.01 and 0.02, F values [341, 341] = 6.66 and 5.11, respectively). In contrast to the *Christensenellaceae*, both *Methanobacteriaceae* and *Methanobrevibacter* were positively correlated with age (type II ANOVA, respective P values = 0.001 and 4.27×10^{-4} and F values [1,468, 1,468] = 10.35 and 12.47), indicating that older people carry a greater proportion of methanogens. Moreover, *M. smithii*, the most abundant and prevalent methanogen species within the human gut, was also positively correlated with age and negatively with BMI regardless of age; i.e., the interaction term between age and BMI was not significantly correlated (see Appendix 2 in Text S1 for additional statistics).

The relative abundances of the *Christensenella* and *Methanobrevibacter* genera are significantly correlated across populations. Next, we looked into how the *Christensenellaceae* and the *Methanobacteriaceae* correlated with each other across subjects while controlling for BMI and age. We constructed a model where Mf-tra was included in addition to BMI and age (model Cf-Mf). This allowed us to test whether adding Mf-tra to the model improved its fit and, if so, how much of the variance of Cf-tra not explained by age and BMI could be explained by Mf-tra. We also evaluated the interaction terms between Mf-tra and BMI and between Mf-tra and age to assess whether the correlation between Cf-tra and Mf-tra was dependent on age and BMI. The interaction term for BMI and Mf-tra was not significant and was removed from the model; the interaction term for age and Mf-tra was significant and was retained (type I ANOVA, F value [339] = 8.30 and P value = 0.0042). We compared the log likelihoods of the null and full models (Cf-null and Cf-Mf) to confirm that the relative abundances of the *Methanobacteriaceae* and *Christensenellaceae* families were significantly correlated (χ^2 test, P value $= 1.78 \times 10^{-59}$). Furthermore, the model Cf-Mf showed that Mf-tra was significantly positively correlated with Cf-tra (Fig. 1b) (type I ANOVA, F value [339] = 287.03, P value < 0.0001) and that the interaction term between Mf-tra and age was positively correlated with Cf-tra as well. These results indicate that the relative abundances of the *Christensenellaceae* and *Methanobacteriaceae* families are positively correlated across multiple populations/studies. In addition, although both families are enriched in low-BMI people, they are correlated regardless of a subject's BMI. Moreover, their association is stronger in older people, suggesting that although elders are less likely to carry as much *Christensenellaceae* as youths, the more *Methanobacteriaceae* they have, the more *Christensenellaceae* they have.

We performed a similar analysis using the abundances of the two most prominent genera belonging to these families (*Christensenella* and *Methanobrevibacter*, models Cg-null and Cg-Mg) and obtained equivalent results. First, the interaction term between Mg-tra and age was positively correlated with Cg-tra (Fig. 1c) (type I ANOVA, F value [339] = 10.19, P value = 0.0015). Then, by comparing model Cg-null with our full model Cg-Mg, we showed that the relative abundances of the two genera were also correlated (χ^2 test, P value $= 1.50 \times 10^{-57}$). Our full model Cg-Mg showed that Mg-tra was significant for predicting Cg-tra while controlling for BMI and age (type I ANOVA, F value [339] = 274.35, P value < 0.0001), with the interaction term between Mg-tra and age also positively correlating with Cg-tra. These results indicate that the correlations

between the relative abundances of the two families, explained above, hold true at the level of two representative genera. The association between *Methanobrevibacter* and *Christensenella* is stronger in older people regardless of BMI.

A similar analysis at the species level indicated that *C. minuta* and *M. smithii* were the most abundant species of each of their genera, and similarly to the family and genus ranks, their relative abundances across samples were significantly correlated (Fig. 1d and Appendix 2 in Text S1). The less abundant *Christensenella* gut species *C. massiliensis* and *C. timonensis* also correlated with *Methanobrevibacter smithii* across the 1,821 metagenomes (see Appendix 2 in Text S1). *C. minuta* and *C. timonensis*'s transformed relative abundances were significantly negatively correlated with both BMI and age, while *C. massiliensis*'s transformed relative abundance was significantly correlated with BMI but not with age. Leaner people are thus enriched in members of the *Christensenellaceae* family, and *C. minuta* and *C. timonensis* are more abundant in young people than in older people.

***C. minuta* forms flocs alone and in coculture with *M. smithii*.** To assess the physical and metabolic interactions of two representative species, we used *C. minuta* DSM-22607, previously shown to reduce adiposity in germfree mouse fecal transplant experiments (4), and *M. smithii* DSM-861, which is the most abundant and prevalent methanogen in the human gut (31). Confocal and scanning electron imaging of 2- to 7-day-old cultures revealed that *C. minuta* organisms flocculate in mono- and cocultures (Fig. 2a and b and Fig. 3a to c and g to j). *M. smithii* is present within the *C. minuta* flocs (Fig. 2d and Fig. 3g to j) but does not aggregate in monoculture before 7 to 10 days of culture (data not shown). In contrast, *B. thetaiotaomicron*, used here as a positive control based on previous reports that it supports the growth of *M. smithii* via H_2 production (25, 26), did not flocculate when grown alone (Fig. 2c) and, when cocultured with *M. smithii*, displayed very limited aggregation (Fig. 2e, Fig. 3k to n, and Fig. S2).

H_2 and CH_4 production. After 6 days in monoculture, *C. minuta* had produced 7 times more H_2 than *B. thetaiotaomicron* (14.2 ± 1.6 mmol · liter^{-1} versus 2.0 ± 0.0 mmol · liter^{-1}) (Fig. 4a and d and Fig. 5a; Wilcoxon rank sum test, P value = 0.1). As expected, *M. smithii* did not grow in monoculture when H_2 was not supplied (80:20, vol/vol, N_2-CO_2 headspace) (Fig. 4b). After 6 days, *M. smithii* had produced 9.0 ± 1.0 mmol · liter^{-1} of CH_4 when H_2 was provided in excess (i.e., 80:20, vol/vol, H_2-CO_2 atmosphere at 2×10^5 Pa) (Fig. 4b and Fig. 5b).

In accordance with the higher levels of H_2 produced by *C. minuta* than by *B. thetaiotaomicron*, day 6 CH_4 concentrations were higher for *M. smithii* cocultured with *C. minuta* than with *B. thetaiotaomicron* (respectively, 5.8 ± 0.5 mmol · liter^{-1} and 1.1 ± 0.0 mmol · liter^{-1}; Wilcoxon rank sum test, P value = 0.1) (Fig. 4c and e and Fig. 5b). For both coculture conditions, H_2 concentrations were very low (on average, across time points and replicates, H_2 concentrations were 0.5 ± 0.6 mmol · liter^{-1} in cocultures with *C. minuta* and 0.1 ± 0.1 mmol · liter^{-1} in cocultures with *B. thetaiotaomicron*), indicating that almost all the H_2 that had been produced was also consumed (Fig. 4c and e and Fig. 5a).

Pressure effects on gas production and aggregation. Gas-consuming microbes, including hydrogenotrophic methanogens, grow better in a pressurized environment (32–34) due to a higher gas solubility at higher pressure, as described by Henry's law. We compared levels of CH_4 production by *M. smithii* in monoculture and in coculture with *C. minuta* under 2 different pressures (i.e., 2×10^5 Pa and atmospheric pressure). As with their flocculation at 2×10^5 Pa (Fig. 2d), *C. minuta* and *M. smithii* aggregated at atmospheric pressure (Fig. S3a and b). Accordingly, *C. minuta* supported CH_4 production by *M. smithii* to similar extents under both pressure conditions (ANOVA followed by Tukey's *post hoc* test, adjusted P value = 1.0) (Fig. 4c and 5b), even though the putative H_2 produced by *C. minuta* (estimated based on the monocultures) was much lower than the amount of H_2 provided in the headspace for *M. smithii* (Fig. 5a).

We next sought to assess whether the mixed aggregation of *M. smithii* with *C. minuta* could be disrupted if H_2 was pressurized in the medium, reducing *M. smithii*'s

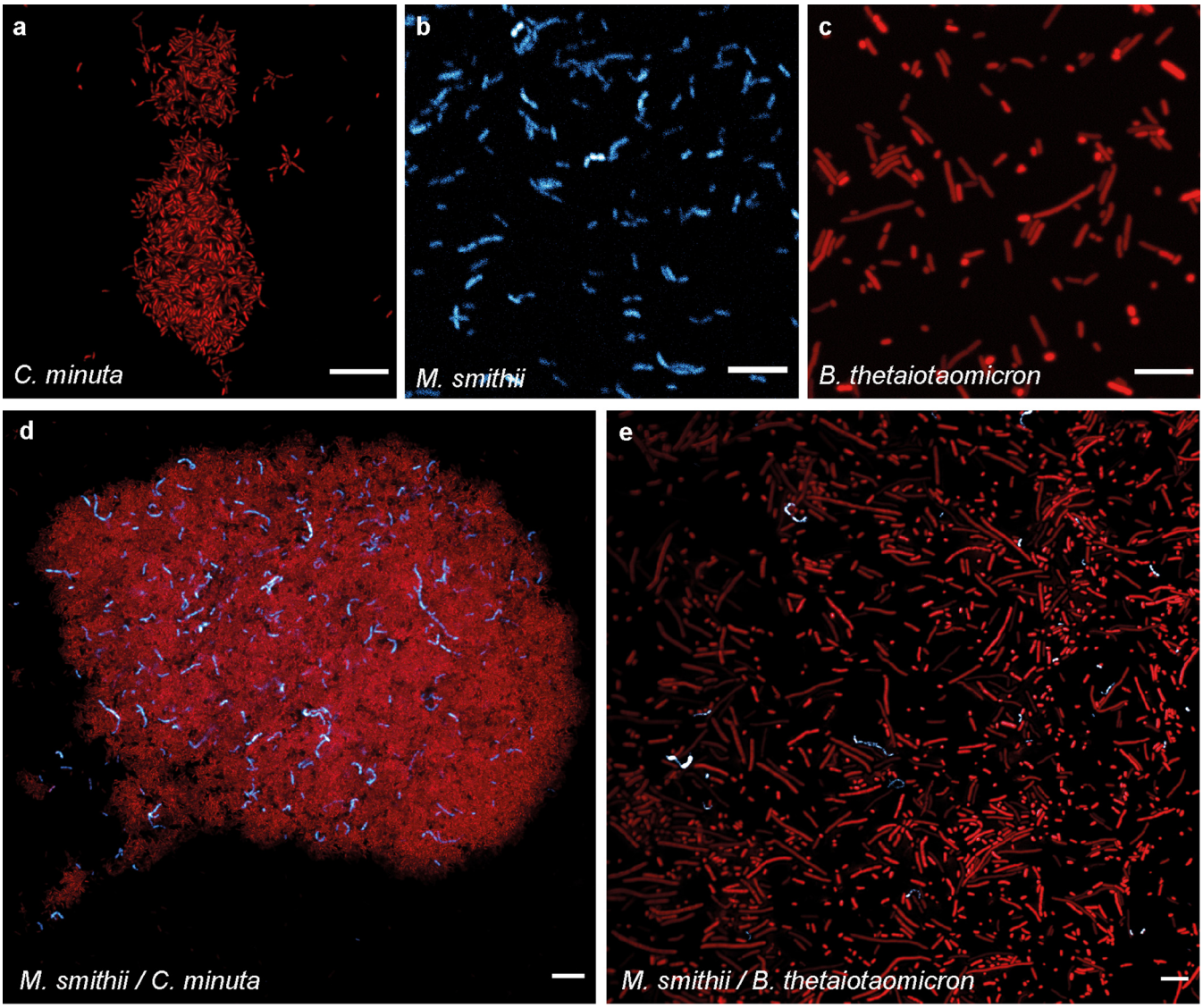

FIG 2 Confocal micrographs of the cultures after 3 days of growth. (a) *C. minuta* alone; (b) *M. smithii* alone; (c) *B. thetaiotaomicron* alone; (d) *M. smithii* and *C. minuta* together; (e) *M. smithii* and *B. thetaiotaomicron* together. SYBR green I fluorescence (DNA staining) is shown in red, and *M. smithii*'s coenzyme F_{420} autofluorescence is shown in blue. Scale bars represent 10 μm. Based on gas production, at 3 days of growth, *B. thetaiotaomicron* was already at stationary phase (explaining the elongated cells) (see Fig. S2 for confocal micrographs of *B. thetaiotaomicron* and *M. smithii* at 2 days of growth), *C. minuta* was at the end of the exponential phase, and *M. smithii* was still in exponential phase.

reliance on *C. minuta* as a H_2 source. We observed that *M. smithii* aggregated with *C. minuta* (Fig. S3c and d) even though H_2 was abundant. Total CH_4 production was higher than in monocultures under the same headspace, reaching 14.2 $\pm$ 5.3 mmol $\cdot$ liter^{-1} in coculture versus 9.0 $\pm$ 1.0 mmol $\cdot$ liter^{-1} in monoculture after 6 days (ANOVA followed by Tukey's *post hoc* test, adjusted *P* value = 0.1) (Fig. 4b and c). This indicates that interspecies H_2 transfer occurs even when H_2 is added to the headspace and leads to greater methanogenesis.

The SCFA production of *C. minuta* is influenced by the presence of *M. smithii*. Regardless of headspace composition and pressure conditions, the only short-chain fatty acids (SCFAs) detected as produced by *C. minuta* in monoculture were acetate and butyrate (among 10 short and medium-chain fatty acids analyzed) (see Appendix 1 in Text S1 and Fig. 5). To investigate if the consumption of H_2 by *M. smithii* influenced the SCFA production profile of *C. minuta*, we compared acetate and butyrate concentrations between the cocultures and *C. minuta*'s monocultures under all conditions tested

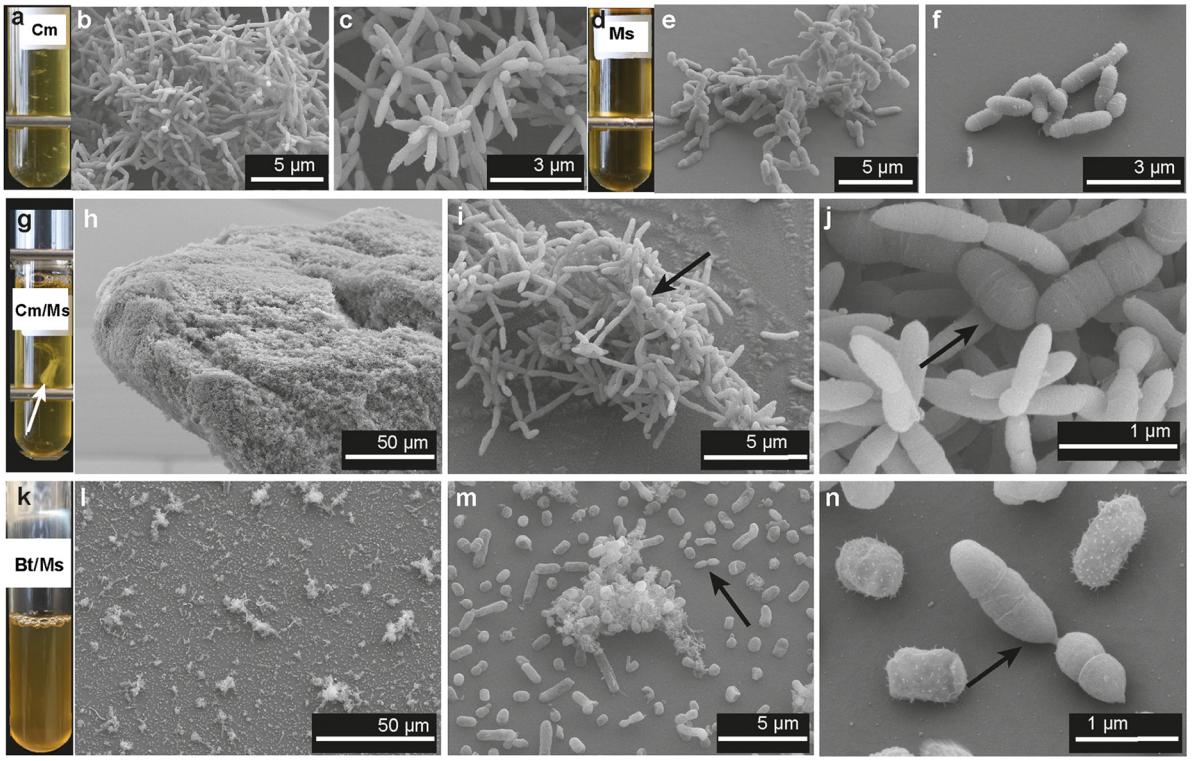

FIG 3 Scanning electron micrographs of the cultures at 3 to 7 days of growth. (a, d, g, and k) Representative Balch tubes of cultures of *C. minuta* (Cm), *M. smithii* (Ms), *C. minuta* and *M. smithii* (Cm/Ms), and *B. thetaiotaomicron* and *M. smithii* (Bt/Ms) after 7 days of growth; (b and c) scanning electron micrographs (SEMs) of monocultures of *C. minuta* at 5 days of growth; (e and f) SEMs of monocultures of *M. smithii* at 5 days of growth; (h to j) SEMs of cocultures of *C. minuta* and *M. smithii* at 7, 5, and 2 days of growth, respectively; (l to n) SEMs of cocultures of *B. thetaiotaomicron* and *M. smithii* at 7 days of growth. The floc formed by *C. minuta* and *M. smithii* is indicated with a white arrow in panel g; other arrows indicate *M. smithii* cells. Metal bars in panels a, d, and g are from the tube rack.

(i.e., cultures at 2×10^5 Pa or atmospheric pressure with an 80:20, vol/vol, N_2-CO_2 or H_2-CO_2 headspace (Table S1).

We consistently observed lower butyrate concentrations in all cocultures than in monocultures (Fig. 6a to c and 5c) (ANOVA, F value [1] = 161.461 and adjusted P value = 7.7×10^{-8}). For all conditions, butyrate concentrations in coculture after 6 days were 1.1 ± 0.24 mmol · liter^{-1} lower than in monocultures (Fig. 6a to c and Table

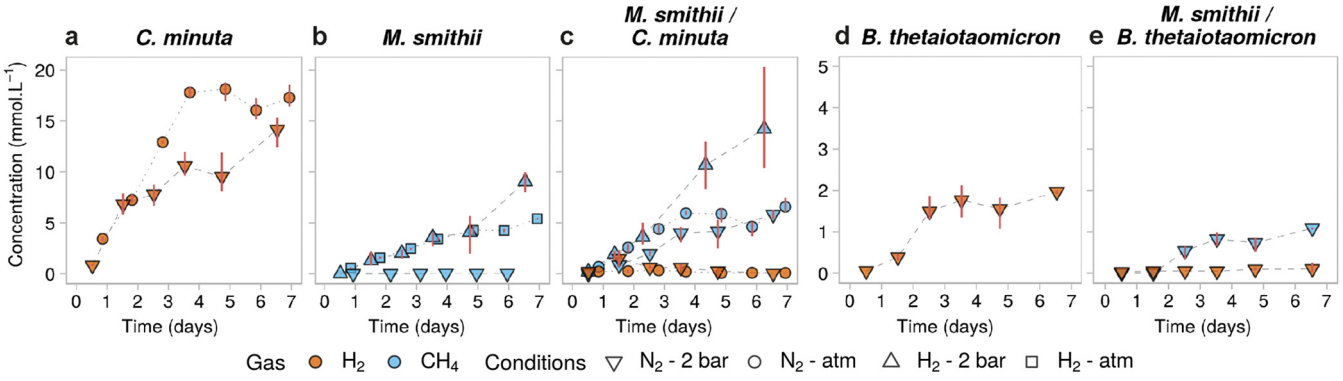

FIG 4 Gas concentrations over time in mono- and cocultures of *C. minuta*, *B. thetaiotaomicron*, and *M. smithii* grown under different conditions. (a to e) H_2 (orange) and CH_4 (blue) concentrations in the headspace over time in cultures from batches 1 to 3 (Table S1). Points represent the averages of results from 3 biological replicates for each condition, and red bars join the minimal and maximal values. In conditions where H_2 was provided in excess (H_2, 2×10^5 Pa, and atmospheric (atm) H_2, with the headspace initially composed of 80:20, vol/vol, H_2-CO_2), its concentrations are not shown for scale reasons. Initial concentrations of H_2 under conditions where it was not provided in the headspace were undetectable (N_2, 2×10^5 Pa, and atmospheric N_2, with the headspace initially composed of 80:20, vol/vol, N_2-CO_2) and stayed null in the monocultures of *M. smithii* (not shown). CH_4 concentrations in the bacterial monocultures were undetectable and are not shown as well. (a to c) Same y scale as in panels d and e.

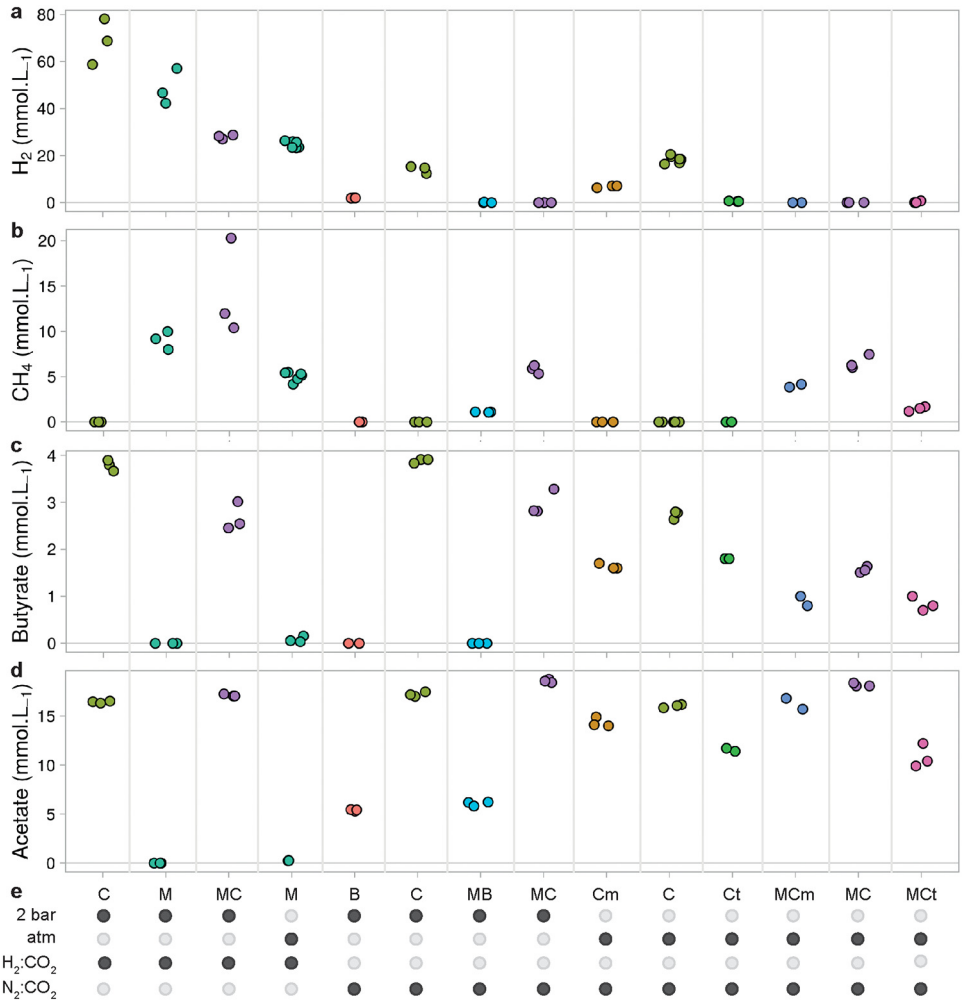

FIG 5 Summary of gases and SCFAs produced in mono- and cocultures of *C. minuta*, *C. timonensis*, *C. massiliensis*, *B. thetaiotaomicron*, and *M. smithii* after 6 days of growth. (a to d) H_2, CH_4, butyrate, and acetate production after 6 days of growth in all mono- and cocultures presented in this study (batches 1 to 4) (Table S1). Points represent the concentration of each biological replicate. (e) Table summarizing the conditions for each culture. The conditions include the gas mixture (H_2-CO_2 or N_2-CO_2 at 80:20, vol/vol), the initial pressure (2×10^5 Pa or atmospheric), and the microorganisms inoculated. C, *C. minuta*; Ct, *C. timonensis*; Cm, *C. massiliensis*; B, *B. thetaiotaomicron*; M, *M. smithii*; MC, *M. smithii* and *C. minuta*; MB, *M. smithii* and *B. thetaiotaomicron*; MCm, *M. smithii* and *C. massiliensis*; MCt, *M. smithii* and *C. timonensis*. Samples inoculated with the same microorganisms are the same color.

A3 in Text S1). The interaction factor between the mono/coculture conditions and the growth condition was not significantly correlated with butyrate concentrations (ANOVA, F value [2] = 0.862, adjusted P value = 0.4). The observation that butyrate concentrations in cocultures were lower than in monocultures regardless of pressure and headspace composition suggest that the methanogen's presence shapes the metabolite output of *C. minuta*.

We observed, along with the reduced butyrate production, slightly but significantly higher acetate production in cocultures than in monocultures (Fig. 6d to f and 5d) (ANOVA, F value [1] = 317.41 and adjusted P value = 3.2×10^{-9}). This difference was also observed in three additional batches performed at 2×10^5 Pa (Fig. S4). The differences in acetate production between mono- and coculture conditions significantly varied with the headspace and pressure conditions (the interaction term between the mono- or coculture and the growth condition was significantly correlated with acetate production; ANOVA, F value [2] = 29.09 and adjusted P value = 3.0×10^{-5}). The differences in final acetate production (after 6 days) ranged

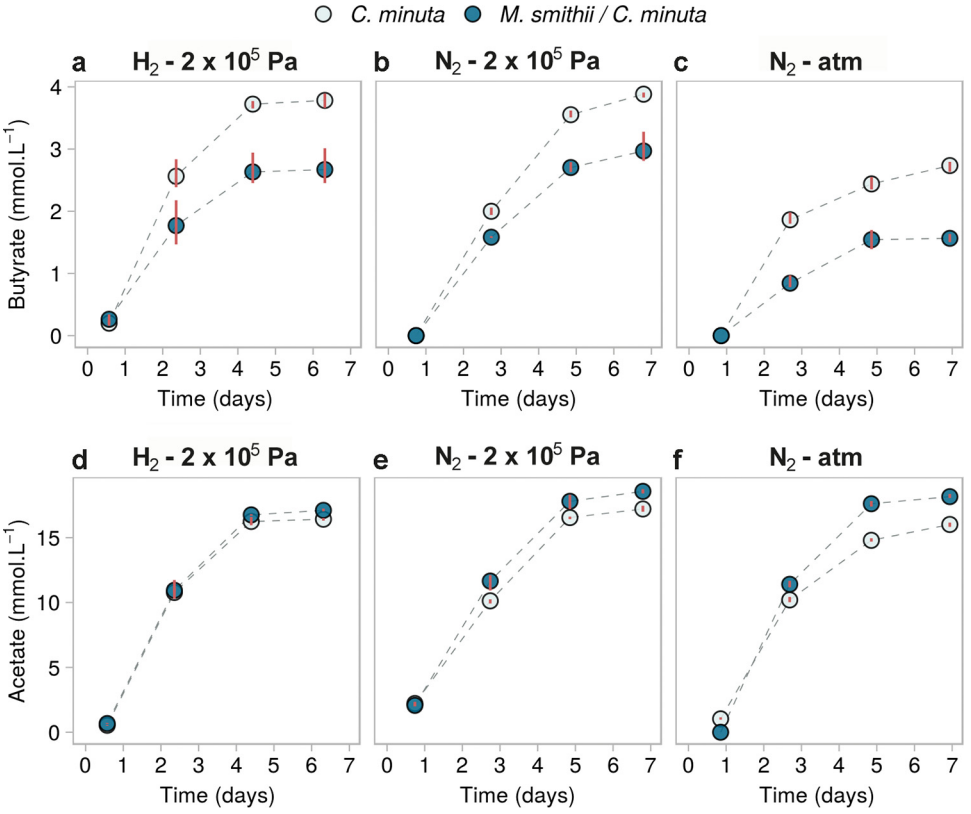

FIG 6 SCFA concentrations over time in mono- and cocultures of *C. minuta* and *M. smithii* grown under different conditions and in cultures from batches 1 to 3 (Table S1). (a to c) Butyrate concentrations; (d to f) acetate concentrations. Only these SCFAs were detected among the fatty acids tested (fatty acids from C_1 to C_8, iso-valerate, and iso-butyrate). Points represent the averages of results from 3 biological replicates for each condition, and red bars join the minimal and maximal values. Monocultures of *M. smithii* are not shown, as they did not differ from the blanks (negative controls).

from $+0.7$ mmol · liter^{-1} at 2×10^5 Pa under a H_2-CO_2 (80:20, vol/vol) atmosphere to $+2.2$ mmol · liter^{-1} at atmospheric pressure under a N_2-CO_2 (80:20, vol/vol) atmosphere. Furthermore, we observed in coculture more CH_4 than what *M. smithii* could have produced based on the H_2 production in *C. minuta*'s monocultures (see Appendix 3 in Text S1). This observation implies that *C. minuta* likely produced a greater amount of H_2 in the cocultures, along with greater acetate production, than in monocultures.

***C. massiliensis and C. timonensis* also support the metabolism of *M. smithii*.** We performed similar coculture experiments of *M. smithii* with *C. massiliensis* and *C. timonensis* at atmospheric pressure. *C. massiliensis* and *C. timonensis* aggregated in monoculture, and *M. smithii* grew within its flocs in coculture (Fig. 7). The H_2 produced

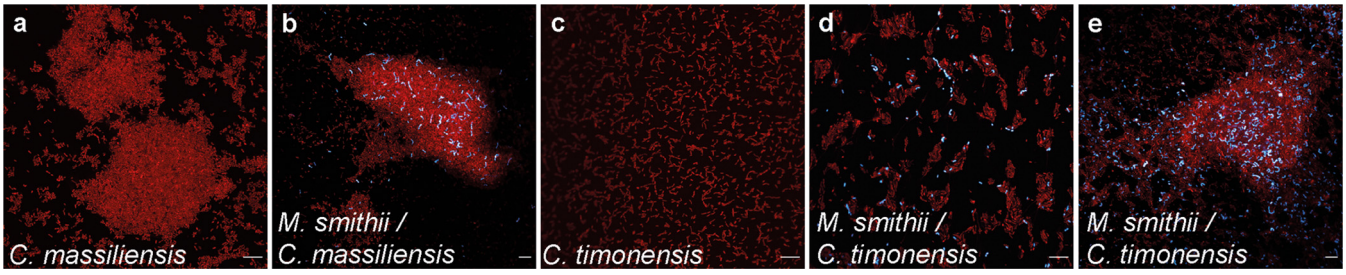

FIG 7 Confocal imaging of *C. massiliensis* and *C. timonensis* in mono- and cocultures with *M. smithii*. Confocal micrographs after 5 days of growth of *C. massiliensis* (a), *M. smithii* and *C. massiliensis* in coculture (b), *C. timonensis* (c), and *M. smithii* and *C. timonensis* in coculture (d and e). SYBR green I fluorescence (DNA staining) is shown in red, and *M. smithii*'s coenzyme F420 autofluorescence is shown in blue. Scale bars represent 10 μm.

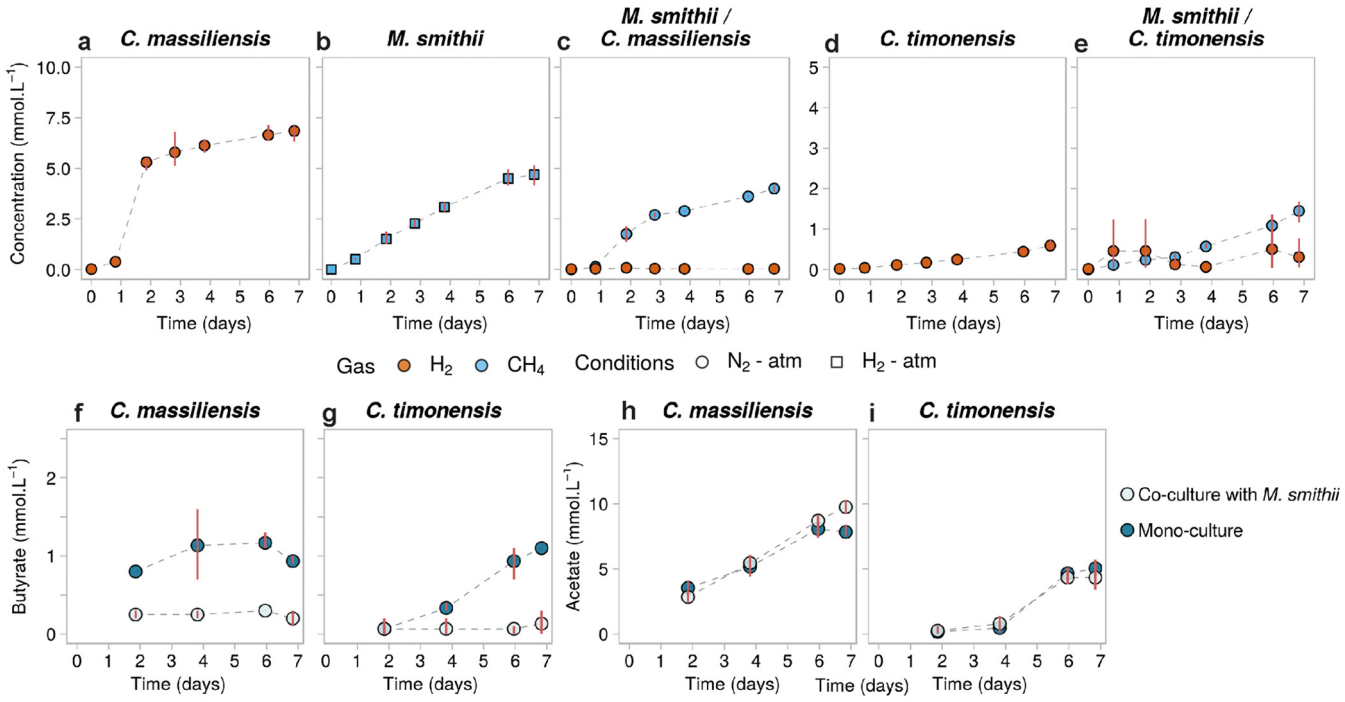

FIG 8 Gas and SCFA concentrations in mono- and cocultures of *C. massiliensis* and *C. timonensis* with *M. smithii*. (a to e) H_2 (orange) and CH_4 (blue) concentrations in the headspace of cultures from batch 4 (Table S1); (f to i) butyrate (f and g) and acetate (h and i) concentrations in these cultures. Points represent the averages of results of 3 biological replicates, and red bars join the minimal and maximal values. (b) In the monocultures of *M. smithii* where H_2 was provided in excess (condition, H_2 atmosphere, with the headspace initially composed of 80:20, vol/vol, H_2-CO_2), its concentrations are not shown for scale reasons.

by the bacteria in monoculture after 6 days of growth (6.9 ± 0.5 mmol · liter^{-1} for *C. massiliensis* and 0.6 ± 0.1 mmol · liter^{-1} for *C. timonensis*) (Fig. 8a and d) was lower than the levels produced by *C. minuta* (Fig. 4a). CH_4 production in the cocultures reached 4.0 ± 0.2 mmol · liter^{-1} with *C. massiliensis* and 1.5 ± 0.3 mmol · liter^{-1} with *C. timonensis*. These amounts of methane are significantly lower than what we observed for *M. smithii* with *C. minuta* (6.6 ± 0.8 mmol · liter^{-1}; ANOVA followed by a Tukey's *post hoc* test, adjusted *P* values = 6.8×10^{-2} and 1.7×10^{-3} for cocultures, respectively, with *C. massiliensis* and *C. timonensis* against *C. minuta*) (Fig. 4c and 8c and e).

We observed less butyrate production in the cocultures than in the monocultures (Wilcoxon rank sum test, *P* values = 0.33 for *C. massiliensis* and 0.5 for *C. timonensis*) (Fig. 8f and g), with butyrate measured barely above the detection limit in cocultures. While in monocultures, *C. massiliensis* and *C. timonensis* produced 0.93 ± 0.06 mmol · liter^{-1} and 1.10 ± 0.00 mmol · liter^{-1} of butyrate, respectively; in coculture with *M. smithii*, they produced 0.20 ± 0.14 mmol · liter^{-1} and 0.13 ± 0.15 mmol · liter^{-1}, respectively. Acetate production by *C. massiliensis* was higher in coculture than in monoculture (7.83 ± 0.49 mmol · liter^{-1} of acetate produced in monoculture by day 6 and 9.75 ± 0.78 mmol · liter^{-1} produced in coculture with *M. smithii*), although this difference was not significant (Wilcoxon rank sum test, *P* value = 0.2). And in contrast with the cocultures of *C. minuta* with *M. smithii*, acetate production by *C. timonensis* was not higher in the cocultures than in monocultures: *C. timonensis* produced 5.05 ± 0.21 mmol · liter^{-1} in monoculture and 4.33 ± 1.21 mmol · liter^{-1} in coculture (Wilcoxon rank sum test, *P* value = 0.8) (Fig. 8h and i).

DISCUSSION

The link between the relative abundance of the *Christensenellaceae* and host BMI now stands as one of the most reproducible associations described between the gut microbiome and obesity (4–15). Here, we confirm in a meta-analysis of metagenomes across 10 populations the previously observed association between leanness and the

Christensenellaceae family (4, 20–22). We could also show that the *Christensenella* genus and *Christensenella* spp. also correlated with leanness. Similarly, we observed correlations between leanness and the *Methanobacteriaceae* family, the *Methanobrevibacter* genus, and *M. smithii*. These methanogens were positively correlated with members of the *Christensenellaceae* family. The relative abundances of the *Christensenellaceae* were higher in young people, whereas conversely, *Methanobacteriaceae* were enriched in older people. Despite these opposite patterns, the two families correlate with each other regardless of age and BMI.

We selected the two most prominent members of the two families, *C. minuta* and *M. smithii*, to ask if physical and metabolic interactions may underlie these positive associations. *C. minuta* produced copious amounts of H_2 during fermentation. In coculture with *C. minuta*, *M. smithii* produced amounts of CH_4 comparable to those in monoculture with an excess of H_2, indicating that *C. minuta* can efficiently support the growth of *M. smithii* via interspecies H_2 transfer. *C. minuta* formed flocs visible by eye, and *M. smithii* grew within these flocs.

M. smithii would likely benefit by associating with the flocs formed by *C. minuta* through better access to H_2. Interspecies metabolite transfer corresponds to the diffusion of a metabolite (e.g., H_2) from the producer (e.g., *C. minuta*) to the consumer (e.g., *M. smithii*). As described by Fick's law of diffusion, the flux of a metabolite between two microorganisms is directly proportional to the concentration gradient and inversely proportional to the distance, such that the closer the microorganisms are, the better the H_2 transfer (35, 36). Thus, within the flocs, the H_2 interspecies transfer would be more efficient, to the benefit of *M. smithii*. In accord, we observed greater methane production under excess H_2 when *C. minuta* was present.

When grown in coculture, *M. smithii* influenced the metabolism of *C. minuta*. The presence of the methanogen inhibited the production of butyrate while enhancing acetate production by *C. minuta* under all growth conditions, on average among all experimental batches. This observation suggests that H_2 consumption by *M. smithii* decreased the P_{H2} within the floc enough to favor acetate production (37). The consumption of H_2 causes the cell to produce more oxidized fermentation products, such as acetate (38–41), and the interspecies H_2 transfer leads to greater CH_4 production.

Both the methane production and the coflocculation were far more pronounced when *M. smithii* was grown with *C. minuta* than with *B. thetaiotaomicron*. *B. thetaiotaomicron* has previously been shown to support the growth of *M. smithii* in coculture (25, 26). *B. thetaiotaomicron* barely aggregated, in contrast to *C. minuta*'s very large (visible to the naked eye) flocs. When grown together, *B. thetaiotaomicron* and *M. smithii* showed very poor aggregation. Moreover, acetate was the only SCFA detected in monocultures of *B. thetaiotaomicron*, and its production was less affected by the methanogen than in *C. minuta*. Methane produced by *M. smithii* in coculture with *B. thetaiotaomicron* was one-fifth of that produced with *C. minuta*, possibly as a result of the smaller amount of H_2 produced and the reduced contact between cells. Given that *M. smithii* does not cooccur with *B. thetaiotaomicron* in human microbiome data sets, this is another indication that cooccurrence patterns may point to metabolic interactions.

C. massiliensis and *C. timonensis* also produced H_2, acetate, and butyrate and also flocculated in monoculture. *C. massiliensis* and *C. timonensis* supported methane production by *M. smithii*, which grew within the bacterial flocs. However, *M. smithii* also grew outside the flocs when cocultured with these two species, which we did not observe in the cocultures with *C. minuta*, and although *M. smithii* also influenced the fermentation of *C. massiliensis* and *C. timonensis*, the overall changes in SCFA production in coculture were different from what we observed with *C. minuta*: butyrate production was almost undetectable, while acetate production was not significantly affected.

These results suggest that the interaction between *M. smithii* and *C. minuta* leads to higher methane production than with *B. thetaiotaomicron* and other species of the

Christensenellaceae, possibly due to the higher levels of interspecies H_2 transfer. Nevertheless, *C. massiliensis* and *C. timonensis* supported CH_4 production better than *B. thetaiotaomicron* did. The higher H_2 production of *C. massiliensis* than of *B. thetaiotaomicron* might explain this. In the case of *C. timonensis*, although it produced half the H_2 produced by *B. thetaiotaomicron* in monoculture, *M. smithii* produced more CH_4 in coculture with *C. timonensis* than with *B. thetaiotaomicron*. This suggests that, as with its effect on *C. minuta*, *M. smithii* triggered the production of H_2 by *C. timonensis*.

Altogether, our work demonstrates that members of the *Christensenellaceae* act as a H_2 source to methanogens, and this process is enhanced via close physical proximity. Such interactions also likely underlie the cooccurrence patterns of the *Christensenellaceae* with other members of the microbiome. Many of these families lack cultured representatives, such as *Firmicutes* unclassified SHA-98, *Tenericutes* unclassified RF39, and unclassified ML615J-28 (4). Based on our results, cultivation of these elusive members of the microbiome may require H_2 (or the provision of another metabolite that *C. minuta* produces when H_2 is being consumed). Despite their very low abundance in the human gut, members of the *Christensenellaceae* may shape the composition of the gut microbiome by favoring the colonization and persistence of certain hydrogenotrophs and by supplying other butyrate producers with acetate (42).

Here, we confirmed an association of *M. smithii* and leanness based on metagenomes from 10 studies. In contrast, some studies have reported an association between *M. smithii* and obesity (2, 43). In this scenario, H_2 uptake by *M. smithii* would promote the breakdown of nondigestible carbon sources by fermenters, such as acetogens, thereby increasing the amount of acetate or other SCFAs that can be absorbed and utilized by the host and promoting fat storage (2, 44). In contrast, and consistently with our results, *M. smithii* has also been repeatedly associated with anorexia and leanness (4, 45–48). In this case, the production of CH_4 would decrease the amount of energy available for the host via carbon loss, as has been observed in livestock (49–52). Thus, our observation that the presence of *M. smithii* directs the metabolic output of the *C. minuta* toward greater H_2 availability for methanogenesis via increased acetate production is consistent with their association with a lean phenotype. To assess quantitatively how the presence and activity of these microbes impact host physiology will require careful modeling of energy flow *in vivo*.

MATERIALS AND METHODS

Metagenome data generation. We generated 141 metagenomes from fecal samples obtained as part of a previous study (53) (see Table S2 in the supplemental material). Metagenomic libraries were prepared as described in Appendix 1 (additional methods) in Text S1.

Data from public databases. We constructed a metagenome sequence collection from (i) the newly generated data (above) to complement the 146 metagenomes previously reported by Poole et al. in 2019 (53) and (ii) publicly available shotgun-metagenome sequences from stool samples included in the curatedMetagenomicData package of Bioconductor (54) for which BMI information was provided. For the latter, we restricted our analyses to individuals for which the following information was available: gender, age, country of origin, and BMI. Individuals with *Schistosoma* ($n = 4$) or Wilson's disease ($n = 2$) were excluded from the analysis, as were samples from two pregnant women. In all, 1,534 samples from 9 studies were downloaded from the sequence read archive (SRA) and further processed (Table S3), for a total or 1,821 samples with at least 1 million sequence pairs per sample.

Data processing. A detailed description of the processing of the raw sequences is given in Appendix 1 in Text S1. To obtain a taxonomic profile of the metagenome samples, we built a custom genome database (55) for Kraken v2.0.7 (56) and Bracken v2.2 (57) using the representative genomes from the proGenomes database (as available on 24 August 2018) (58), to which we added genome sequences of *C. minuta* (GenBank assembly accession number GCA_001652705.1), *C. massiliensis* (GCA_900155415.1), and *C. timonensis* (GCA_900087015.1). Reads were classified using Kraken2, and a Bayesian reestimation of the species-level abundance of each sample was then performed using Bracken2. We obtained complete taxonomic annotations from NCBI taxon IDs with TaxonKit v0.2.4 (https://bioinf.shenwei.me/taxonkit/). The detection limit for the relative abundances in samples was 10^{-3}%; in consequence, all relative abundances below this threshold were equal to 0.

Meta-analysis of human gut metagenomes. Linear mixed models (R package nlme) were used to evaluate the correlation between the relative abundances of taxa while correcting for the structure of the population; the study of origin was set as a random effect. In some data sets, individuals were sampled multiple times, in which case the individual effect was nested inside the data set effect. Relative

abundances were transformed using Tukey's ladder of power transformation (59) and are designated with the suffix "-tra" (e.g., the transformed relative abundance of the family *Christensenellaceae* is Cf-tra). Covariates in null models were selected using a backward feature selection approach based on a type II ANOVA (i.e., by including all covariates and removing the nonsignificant ones step-by-step until all remaining variables were significant [see Appendix 2 in Text S1). We made 4 null models predicting the transformed relative abundances of members of the family *Christensenellaceae* (Cf-null), the genus *Christensenella* (Cg-null), the family *Methanobacteriaceae* (Mf-null), and the genus *Methanobrevibacter* (Mg-null). To evaluate the correlation between taxa, we made model Cf-Mf by adding Mf-tra and its interaction with age to the covariates of Cf-null. Reciprocally, we made model Cg-Mg by adding Mg-tra and its interaction with age to the covariates of Cg-null. The same approach was performed at the species level, and it is described in Appendix 2 in Text S1.

$$\text{For Cf-null, Cf-tra} = \text{BMI} + \text{age} + 1|\text{data set/individual}$$

$$\text{For Cg-null, Cg-tra} = \text{BMI} + \text{age} + 1|\text{data set/individual}$$

$$\text{For Mf-null, Mf-tra} = \text{BMI} + \text{age} + 1|\text{data set/individual}$$

$$\text{For Mg-null, Mg-tra} = \text{BMI} + \text{age} + 1|\text{data set/individual}$$

$$\text{For Cf-Mf, Cf-tra} = \text{BMI} + \text{age} + \text{Mf-tra} + \text{age} \times \text{Mf-tra} + 1|\text{data set/individual}$$

$$\text{For Cg-Mg, Cg-tra} = \text{BMI} + \text{age} + \text{Mg-tra} + \text{age} \times \text{Mg-tra} + 1|\text{data set/individual}$$

We used the likelihood ratio test to compare the nested models via the χ^2 distribution (i.e., Cf-null versus Cf-Mf and Cg-null versus Cg-Mg). To characterize the correlation of Cf-tra with Mf-tra and Cg-tra with Mg-tra, after correcting for BMI and age, we used a type I ANOVA to evaluate the importance of the variables in the order in which they appear in Cf-Mf and Cg-Mg. The *F* value, degree of freedom, and *P* value are reported for each variable. All analyses were performed using R (60).

Culturing of methanogens and bacteria. We obtained *M. smithii* DSM-861, *C. minuta* DSM-22607, *C. massiliensis* DSM 102344, *C. timonensis* DSM 102800, and *B. thetaiotaomicron* VPI-5482 from the German Collection of Microorganisms and Cell Cultures (DSMZ; Braunschweig, Germany). Each culture was thawed and inoculated into brain heart infusion (BHI) medium (Carl Roth, Karlsruhe, Germany) supplemented with yeast extract (5 g/liter), reduced with L-cysteine-HCl (0.5 g/liter) and Ti-NTA III (0.3 mM), and buffered with sodium bicarbonate (42 mM, pH 7, adjusted with HCl 6 M). Cultures (10 ml) were grown at 37°C without shaking in Balch tubes (total volume of 28 ml) under a headspace of N_2-CO_2 (80:20, vol/vol) in the case of the bacteria and H_2-CO_2 (80:20, vol/vol, with pressure adjusted to 2×10^5 Pa) for *M. smithii*. When initial cultures reached exponential growth and before floc formation, they were transferred into fresh medium, and these transfers were used as inocula for the experiments described below.

Coculture conditions. *M. smithii* was cocultured with *C. minuta*, *B. thetaiotaomicron*, *C. massiliensis*, or *C. timonensis*, and in parallel, each microorganism was grown in monoculture (Table S1). Prior to inoculation, 1-day-old cultures of bacterial species or 4-day-old cultures of *M. smithii* were adjusted to an optical density at 600 nm (OD_{600}) of 0.01 with sterile medium. For the cocultures, 0.5 ml of each adjusted culture was inoculated into 9 ml of fresh medium. For the monocultures, 0.5 ml of the adjusted culture and 0.5 ml of sterile medium were combined as an inoculum. For negative controls, sterile medium was transferred as a mock inoculum. Headspaces were exchanged with 80:20 (vol/vol) N_2-CO_2 or H_2-CO_2 and pressurized at 2×10^5 Pa or atmospheric pressure (Table S1). Each batch of experiments was carried out once with 3 biological replicates per culture condition (Table S1).

Imaging. For confocal microscopy, SYBR green I staining was performed as previously described (61) with the modifications described in Appendix 1 in Text S1. Imaging by confocal microscopy (LSM 780 NLO; Zeiss) was used to detect the autofluorescence emission of coenzyme F_{420} of *M. smithii* and the emission of SYBR green I (Appendix 1 in Text S1). Images were acquired with the ZEN Black 2.3 SP1 software and processed with FIJI (62). Micrographs are representative of all replicate cultures within each experimental batch. The preparation of the samples for scanning electron microscopy is described in Appendix 1 in Text S1. Cells were examined with a field emission scanning electron microscope (Regulus 8230; Hitachi High Technologies, Tokyo, Japan) at an accelerating voltage of 10 kV.

Gas and SCFA measurements. Headspace concentrations of H_2, CO_2, and CH_4 were measured with a gas chromatograph (GC) (SRI 8610C; SRI Instruments, Torrance, USA) equipped with a packed column at 42°C (0.3-m HaySep-D packed Teflon; Restek, Bellefonte, PA, USA), a thermal conductivity detector (TCD) at 111°C, and a flame ionization detector (FID). The gas production and consumption were estimated from the total pressure in the vials (ECO2 manometer; Keller, Jestetten, Germany) and the gas concentrations in the headspace using the ideal gas equation. The concentrations are given in millimoles of gas in the headspace per liter of culture.

SCFA measurements were performed with liquid samples (0.5 ml) filtered through 0.2-μm-pore-size polyvinylidene fluoride filters (Carl Roth, GmbH, Karlsruhe, Germany). SCFA concentrations were measured with a CBM-20A high-performance liquid chromatography (HPLC) system equipped with an Aminex HPX-87P column (300 by 7.8 mm; Bio-Rad, CA, USA), maintained at 60°C, and a refractive index detector. A sulfuric acid solution (5 mM) was used as the eluent at a flow rate of 0.6 ml/min ($\sim 40 \times 10^5$-Pa column pressure). Calibration curves for acetate and butyrate were prepared from 1.25 to 50 mM using acetic acid and butyric acid, respectively (Merck KGaA, Darmstadt, Germany). No other fatty acids were detected (see Appendix 1 in Text S1 [63–69]). The SCFA concentrations were estimated with the Shimadzu LabSolutions software.

Statistical analyses. We used Wilcoxon rank sum tests to compare levels of gas production between cultures after 6 days of growth. We performed ANOVA tests when more than one culture condition (i.e., headspace composition and pressure) (Table S1) was included in the comparison. The conditions in the ANOVA tests (i.e., headspace composition and pressure in mono- or cocultures) were evaluated to explain the variance of CH_4 production after 6 days of growth. A Tukey *post hoc* test was then performed to discriminate between the effects of the different conditions. SCFA concentrations were compared using a two-way ANOVA where the culture conditions (i.e., headspace composition and pressure) (Table S1) and the sample (mono- and cocultures) were evaluated to explain the variance of butyrate and acetate concentrations after 6 days of growth. *P* values were adjusted using the Benjamini-Hochberg method. Tukey's *post hoc* test was performed to discriminate between the effects of the different conditions. All statistical analyses were done in R using the stats R package.

Data availability. The metagenomic sequence data generated during this study have been deposited in the European Nucleotide Archive under accession number PRJEB34191 (http://www.ebi.ac.uk/ena/data/view/PRJEB34191). The jupyter notebooks and associated data are available at https://github.com/Albabune/Ruaud_EsquivelElizondo.

SUPPLEMENTAL MATERIAL

Supplemental material is available online only.

TEXT S1, DOCX file, 0.01 MB.

FIG S1, PDF file, 2.6 MB.

FIG S2, JPG file, 0.1 MB.

FIG S3, JPG file, 0.2 MB.

FIG S4, PDF file, 1.1 MB.

TABLE S1, PDF file, 0.02 MB.

TABLE S2, PDF file, 0.04 MB.

TABLE S3, PDF file, 0.1 MB.

ACKNOWLEDGMENTS

We are grateful to Monika Temovska, Sophie Maisch, and Iris Holdermann for valuable help. We also thank Daren Heavens for the metagenome library preparation protocol.

This work was supported by the Max Planck Society and the Humboldt Foundation.

REFERENCES

1. Ley RE, Turnbaugh PJ, Klein S, Gordon JI. 2006. Microbial ecology: human gut microbes associated with obesity. Nature 444:1022–1023. https://doi.org/10.1038/4441022a.
2. Turnbaugh PJ, Ley RE, Mahowald MA, Magrini V, Mardis ER, Gordon JI. 2006. An obesity-associated gut microbiome with increased capacity for energy harvest. Nature 444:1027–1031. https://doi.org/10.1038/nature05414.
3. Waters JL, Ley RE. 2019. The human gut bacteria *Christensenellaceae* are widespread, heritable, and associated with health. BMC Biol 17:83. https://doi.org/10.1186/s12915-019-0699-4.
4. Goodrich JK, Waters JL, Poole AC, Sutter JL, Koren O, Blekhman R, Beaumont M, Van Treuren W, Knight R, Bell JT, Spector TD, Clark AG, Ley RE. 2014. Human genetics shape the gut microbiome. Cell 159:789–799. https://doi.org/10.1016/j.cell.2014.09.053.
5. Fu J, Bonder MJ, Cenit MC, Tigchelaar EF, Maatman A, Dekens JAM, Brandsma E, Marczynska J, Imhann F, Weersma RK, Franke L, Poon TW, Xavier RJ, Gevers D, Hofker MH, Wijmenga C, Zhernakova A. 2015. The gut microbiome contributes to a substantial proportion of the variation in blood lipids. Circ Res 117:817–824. https://doi.org/10.1161/CIRCRESAHA.115.306807.
6. Goodrich JK, Davenport ER, Beaumont M, Jackson MA, Knight R, Ober C, Spector TD, Bell JT, Clark AG, Ley RE. 2016. Genetic determinants of the gut microbiome in UK twins. Cell Host Microbe 19:731–743. https://doi.org/10.1016/j.chom.2016.04.017.
7. Kummen M, Holm K, Anmarkrud JA, Nygård S, Vesterhus M, Høivik ML, Trøseid M, Marschall H-U, Schrumpf E, Moum B, Røsjø H, Aukrust P, Karlsen TH, Hov JR. 2017. The gut microbial profile in patients with primary sclerosing cholangitis is distinct from patients with ulcerative colitis without biliary disease and healthy controls. Gut 66:611–619. https://doi.org/10.1136/gutjnl-2015-310500.
8. Lim MY, You HJ, Yoon HS, Kwon B, Lee JY, Lee S, Song Y-M, Lee K, Sung J, Ko G. 2017. The effect of heritability and host genetics on the gut microbiota and metabolic syndrome. Gut 66:1031–1038. https://doi.org/10.1136/gutjnl-2015-311326.
9. Oki K, Toyama M, Banno T, Chonan O, Benno Y, Watanabe K. 2016. Comprehensive analysis of the fecal microbiota of healthy Japanese adults reveals a new bacterial lineage associated with a phenotype characterized by a high frequency of bowel movements and a lean body type. BMC Microbiol 16:284. https://doi.org/10.1186/s12866-016-0898-x.
10. Stanislawski MA, Dabelea D, Wagner BD, Sontag MK, Lozupone CA, Eggesbø M. 2017. Pre-pregnancy weight, gestational weight gain, and the gut microbiota of mothers and their infants. Microbiome 5:113. https://doi.org/10.1186/s40168-017-0332-0.
11. Yun Y, Kim H-N, Kim SE, Heo SG, Chang Y, Ryu S, Shin H, Kim H-L. 2017. Comparative analysis of gut microbiota associated with body mass index in a large Korean cohort. BMC Microbiol 17:151. https://doi.org/10.1186/s12866-017-1052-0.
12. Brooks AW, Priya S, Blekhman R, Bordenstein SR. 2018. Gut microbiota diversity across ethnicities in the United States. PLoS Biol 16:e2006842. https://doi.org/10.1371/journal.pbio.2006842.
13. Jackson MA, Bonder MJ, Kuncheva Z, Zierer J, Fu J, Kurilshikov A, Wijmenga C, Zhernakova A, Bell JT, Spector TD, Steves CJ. 2018. Detection of stable community structures within gut microbiota co-occurrence networks from different human populations. PeerJ 6:e4303. https://doi.org/10.7717/peerj.4303.
14. López-Contreras BE, Morán-Ramos S, Villarruel-Vázquez R, Macías-Kauffer L, Villamil-Ramírez H, León-Mimila P, Vega-Badillo J, Sánchez-Muñoz F, Llanos-Moreno LE, Canizalez-Román A, Del Río-Navarro B, Ibarra-González I, Vela-Amieva M, Villarreal-Molina T, Ochoa-Leyva A, Aguilar-Salinas CA, Canizales-Quinteros S. 2018. Composition of gut microbiota in obese and normal-weight Mexican school-age children and its association with metabolic traits. Pediatr Obes 13:381–388. https://doi.org/10.1111/ijpo.12262.
15. Peters BA, Shapiro JA, Church TR, Miller G, Trinh-Shevrin C, Yuen E, Friedlander C, Hayes RB, Ahn J. 2018. A taxonomic signature of obesity

in a large study of American adults. Sci Rep 8:9749. https://doi.org/10.1038/s41598-018-28126-1.
16. Morotomi M, Nagai F, Watanabe Y. 2012. Description of *Christensenella minuta* gen. nov., sp. nov., isolated from human faeces, which forms a distinct branch in the order *Clostridiales*, and proposal of *Christensenellaceae* fam. nov. Int J Syst Evol Microbiol 62:144–149. https://doi.org/10.1099/ijs.0.026989-0.
17. Costea PI, Hildebrand F, Arumugam M, Bäckhed F, Blaser MJ, Bushman FD, de Vos WM, Ehrlich SD, Fraser CM, Hattori M, Huttenhower C, Jeffery IB, Knights D, Lewis JD, Ley RE, Ochman H, O'Toole PW, Quince C, Relman DA, Shanahan F, Sunagawa S, Wang J, Weinstock GM, Wu GD, Zeller G, Zhao L, Raes J, Knight R, Bork P. 2018. Enterotypes in the landscape of gut microbial community composition. Nat Microbiol 3:8–16. https://doi.org/10.1038/s41564-017-0072-8.
18. Turpin W, Espin-Garcia O, Xu W, Silverberg MS, Kevans D, Smith MI, Guttman DS, Griffiths A, Panaccione R, Otley A, Xu L, Shestopaloff K, Moreno-Hagelsieb G, GEM Project Research Consortium, Paterson AD, Croitoru K. 2016. Association of host genome with intestinal microbial composition in a large healthy cohort. Nat Genet 48:1413–1417. https://doi.org/10.1038/ng.3693.
19. Bonder MJ, Kurilshikov A, Tigchelaar EF, Mujagic Z, Imhann F, Vila AV, Deelen P, Vatanen T, Schirmer M, Smeekens SP, Zhernakova DV, Jankipersadsing SA, Jaeger M, Oosting M, Cenit MC, Masclee AAM, Swertz MA, Li Y, Kumar V, Joosten L, Harmsen H, Weersma RK, Franke L, Hofker MH, Xavier RJ, Jonkers D, Netea MG, Wijmenga C, Fu J, Zhernakova A. 2016. The effect of host genetics on the gut microbiome. Nat Genet 48:1407–1412. https://doi.org/10.1038/ng.3663.
20. Hansen EE, Lozupone CA, Rey FE, Wu M, Guruge JL, Narra A, Goodfellow J, Zaneveld JR, McDonald DT, Goodrich JA, Heath AC, Knight R, Gordon JI. 2011. Pan-genome of the dominant human gut-associated archaeon, *Methanobrevibacter smithii*, studied in twins. Proc Natl Acad Sci U S A 108(Suppl 1):4599–4606. https://doi.org/10.1073/pnas.1000071108.
21. Upadhyaya B, McCormack L, Fardin-Kia AR, Juenemann R, Nichenametla S, Clapper J, Specker B, Dey M. 2016. Impact of dietary resistant starch type 4 on human gut microbiota and immunometabolic functions. Sci Rep 6:28797. https://doi.org/10.1038/srep28797.
22. Klimenko NS, Tyakht AV, Popenko AS, Vasiliev AS, Altukhov IA, Ischenko DS, Shashkova TI, Efimova DA, Nikogosov DA, Osipenko DA, Musienko SV, Selezneva KS, Baranova A, Kurilshikov AM, Toshchakov SM, Korzhenkov AA, Samarov NI, Shevchenko MA, Tepliuk AV, Alexeev DG. 2018. Microbiome responses to an uncontrolled short-term diet intervention in the frame of the citizen science project. Nutrients 10:576. https://doi.org/10.3390/nu10050576.
23. Vanderhaeghen S, Lacroix C, Schwab C. 2015. Methanogen communities in stools of humans of different age and health status and co-occurrence with bacteria. FEMS Microbiol Lett 362:fnv092. https://doi.org/10.1093/femsle/fnv092.
24. Moore WEC, Johnson JL, Holdeman LV. 1976. Emendation of *Bacteroidaceae* and *Butyrivibrio* and descriptions of *Desulfomonas* gen. nov. and ten new species in the genera *Desulfomonas*, *Butyrivibrio*, *Eubacterium*, *Clostridium*, and *Ruminococcus*. Int J Syst Evol Microbiol 26:238–252. https://doi.org/10.1099/00207713-26-2-238.
25. Traore SI, Khelaifia S, Armstrong N, Lagier JC, Raoult D. 2019. Isolation and culture of *Methanobrevibacter smithii* by coculture with hydrogen-producing bacteria on agar plates. Clin Microbiol Infect 25:1561.e1–1561.e5. https://doi.org/10.1016/j.cmi.2019.04.008.
26. Khelaifia S, Lagier J-C, Nkamga VD, Guilhot E, Drancourt M, Raoult D. 2016. Aerobic culture of methanogenic archaea without an external source of hydrogen. Eur J Clin Microbiol Infect Dis 35:985–991. https://doi.org/10.1007/s10096-016-2627-7.
27. Nkamga VD, Lotte R, Roger P-M, Drancourt M, Ruimy R. 2016. *Methanobrevibacter smithii* and *Bacteroides thetaiotaomicron* cultivated from a chronic paravertebral muscle abscess. Clin Microbiol Infect 22:1008–1009. https://doi.org/10.1016/j.cmi.2016.09.007.
28. Lau SKP, McNabb A, Woo GKS, Hoang L, Fung AMY, Chung LMW, Woo PCY, Yuen K-Y. 2007. *Catabacter hongkongensis* gen. nov., sp. nov., isolated from blood cultures of patients from Hong Kong and Canada. J Clin Microbiol 45:395–401. https://doi.org/10.1128/JCM.01831-06.
29. Rosa BA, Hallsworth-Pepin K, Martin J, Wollam A, Mitreva M. 2017. Genome sequence of *Christensenella minuta* DSM 22607^T. Genome Announc 5:e01451-16. https://doi.org/10.1128/genomeA.01451-16.
30. Hillmann B, Al-Ghalith GA, Shields-Cutler RR, Zhu Q, Gohl DM, Beckman KB, Knight R, Knights D, Hillmann B, Al-Ghalith GA, Shields-Cutler RR, Zhu Q, Gohl DM, Beckman KB, Knight R, Knights D. 2018. Evaluating the information content of shallow shotgun metagenomics. mSystems 3:e00069-18.
31. Gill SR, Pop M, Deboy RT, Eckburg PB, Turnbaugh PJ, Samuel BS, Gordon JI, Relman DA, Fraser-Liggett CM, Nelson KE. 2006. Metagenomic analysis of the human distal gut microbiome. Science 312:1355–1359. https://doi.org/10.1126/science.1124234.
32. Dridi B, Raoult D, Drancourt M. 2011. Archaea as emerging organisms in complex human microbiomes. Anaerobe 17:56–63. https://doi.org/10.1016/j.anaerobe.2011.03.001.
33. Edwards T, McBride BC. 1975. Biosynthesis and degradation of methylmercury in human faeces. Nature 253:463–464. https://doi.org/10.1038/253462a0.
34. Balch WE, Wolfe RS. 1976. New approach to the cultivation of methanogenic bacteria: 2-mercaptoethanesulfonic acid (HS-CoM)-dependent growth of *Methanobacterium ruminantium* in a pressurized atmosphere. Appl Environ Microbiol 32:781–791.
35. Stams AJM, Plugge CM. 2009. Electron transfer in syntrophic communities of anaerobic bacteria and archaea. Nat Rev Microbiol 7:568–577. https://doi.org/10.1038/nrmicro2166.
36. Shen L, Zhao Q, Wu X, Li X, Li Q, Wang Y. 2016. Interspecies electron transfer in syntrophic methanogenic consortia: from cultures to bioreactors. Renew Sustain Energy Rev 54:1358–1367. https://doi.org/10.1016/j.rser.2015.10.102.
37. Angenent LT, Karim K, Al-Dahhan MH, Wrenn BA, Domíguez-Espinosa R. 2004. Production of bioenergy and biochemicals from industrial and agricultural wastewater. Trends Biotechnol 22:477–485. https://doi.org/10.1016/j.tibtech.2004.07.001.
38. Macfarlane S, Macfarlane GT. 2003. Regulation of short-chain fatty acid production. Proc Nutr Soc 62:67–72. https://doi.org/10.1079/PNS2002207.
39. Liu Y, Whitman WB. 2008. Metabolic, phylogenetic, and ecological diversity of the methanogenic *Archaea*. Ann N Y Acad Sci 1125:171–189. https://doi.org/10.1196/annals.1419.019.
40. den Besten G, van Eunen K, Groen AK, Venema K, Reijngoud D-J, Bakker BM. 2013. The role of short-chain fatty acids in the interplay between diet, gut microbiota, and host energy metabolism. J Lipid Res 54:2325–2340. https://doi.org/10.1194/jlr.R036012.
41. Louis P, Flint HJ. 2017. Formation of propionate and butyrate by the human colonic microbiota. Environ Microbiol 19:29–41. https://doi.org/10.1111/1462-2920.13589.
42. Hoyles L, Swann J. 2019. Influence of the human gut microbiome on the metabolic phenotype, p 535–560. *In* Lindon JC, Nicholson JK, Holmes E (ed), The handbook of metabolic phenotyping. Elsevier, Oxford, United Kingdom.
43. Mbakwa CA, Penders J, Savelkoul PH, Thijs C, Dagnelie PC, Mommers M, Arts I. 2015. Gut colonization with *Methanobrevibacter smithii* is associated with childhood weight development. Obesity (Silver Spring) 23:2508–2516. https://doi.org/10.1002/oby.21266.
44. Morrison DJ, Preston T. 2016. Formation of short chain fatty acids by the gut microbiota and their impact on human metabolism. Gut Microbes 7:189–200. https://doi.org/10.1080/19490976.2015.1134082.
45. Mack I, Cuntz U, Grämer C, Niedermaier S, Pohl C, Schwiertz A, Zimmermann K, Zipfel S, Enck P, Penders J. 2016. Weight gain in anorexia nervosa does not ameliorate the faecal microbiota, branched chain fatty acid profiles, and gastrointestinal complaints. Sci Rep 6:26752. https://doi.org/10.1038/srep26752.
46. Armougom F, Henry M, Vialettes B, Raccah D, Raoult D. 2009. Monitoring bacterial community of human gut microbiota reveals an increase in *Lactobacillus* in obese patients and methanogens in anorexic patients. PLoS One 4:e7125. https://doi.org/10.1371/journal.pone.0007125.
47. Million M, Maraninchi M, Henry M, Armougom F, Richet H, Carrieri P, Valero R, Raccah D, Vialettes B, Raoult D. 2012. Obesity-associated gut microbiota is enriched in *Lactobacillus reuteri* and depleted in *Bifidobacterium animalis* and *Methanobrevibacter smithii*. Int J Obes (Lond) 36:817–825. https://doi.org/10.1038/ijo.2011.153.
48. Schwiertz A, Taras D, Schäfer K, Beijer S, Bos NA, Donus C, Hardt PD. 2010. Microbiota and SCFA in lean and overweight healthy subjects. Obesity (Silver Spring) 18:190–195. https://doi.org/10.1038/oby.2009.167.
49. Blaxter KL, Clapperton JL. 1965. Prediction of the amount of methane produced by ruminants. Br J Nutr 19:511–522. https://doi.org/10.1079/bjn19650046.
50. Crutzen PJ, Aselmann I, Seiler W. 1986. Methane production by domestic animals, wild ruminants, other herbivorous fauna, and humans. Tellus B

Chem Phys Meteorol 38B:271–284. https://doi.org/10.1111/j.1600-0889.1986.tb00193.x.
51. Callaway TR, Edrington TS, Rychlik JL, Genovese KJ, Poole TL, Jung YS, Bischoff KM, Anderson RC, Nisbet DJ. 2003. Ionophores: their use as ruminant growth promotants and impact on food safety. Curr Issues Intest Microbiol 4:43–51.
52. Kruger Ben Shabat S, Sasson G, Doron-Faigenboim A, Durman T, Yaacoby S, Berg Miller ME, White BA, Shterzer N, Mizrahi I. 2016. Specific microbiome-dependent mechanisms underlie the energy harvest efficiency of ruminants. ISME J 10:2958–2972. https://doi.org/10.1038/ismej.2016.62.
53. Poole AC, Goodrich JK, Youngblut ND, Luque GG, Ruaud A, Sutter JL, Waters JL, Shi Q, El-Hadidi M, Johnson LM, Bar HY, Huson DH, Booth JG, Ley RE. 2019. Human salivary amylase gene copy number impacts oral and gut microbiomes. Cell Host Microbe 25:553–564.e7. https://doi.org/10.1016/j.chom.2019.03.001.
54. Pasolli E, Schiffer L, Manghi P, Renson A, Obenchain V, Truong DT, Beghini F, Malik F, Ramos M, Dowd JB, Huttenhower C, Morgan M, Segata N, Waldron L. 2017. Accessible, curated metagenomic data through ExperimentHub. Nat Methods 14:1023–1024. https://doi.org/10.1038/nmeth.4468.
55. de la Cuesta-Zuluaga J, Ley RE, Youngblut ND. 2019. Struo: a pipeline for building custom databases for common metagenome profilers. Bioinformatics 2019:btz899. https://doi.org/10.1093/bioinformatics/btz899.
56. Wood DE, Salzberg SL. 2014. Kraken: ultrafast metagenomic sequence classification using exact alignments. Genome Biol 15:R46. https://doi.org/10.1186/gb-2014-15-3-r46.
57. Lu J, Breitwieser FP, Thielen P, Salzberg SL. 2017. Bracken: estimating species abundance in metagenomics data. PeerJ Computer Sci 3:e104. https://doi.org/10.7717/peerj-cs.104.
58. Mende DR, Letunic I, Huerta-Cepas J, Li SS, Forslund K, Sunagawa S, Bork P. 2017. proGenomes: a resource for consistent functional and taxonomic annotations of prokaryotic genomes. Nucleic Acids Res 45:D529–D534. https://doi.org/10.1093/nar/gkw989.
59. Mangiafico SS. 2016. Summary and analysis of extension program evaluation in R, version 1.15.0. Rutgers Cooperative Extension, New Brunswick, NJ. https://rcompanion.org/handbook/.
60. R Core Team. 2017. R: a language and environment for statistical computing. R Foundation for Statistical Computing, Vienna, Austria.
61. Lambrecht J, Cichocki N, Hübschmann T, Koch C, Harms H, Müller S. 2017. Flow cytometric quantification, sorting and sequencing of methanogenic archaea based on F_{420} autofluorescence. Microb Cell Fact 16:180. https://doi.org/10.1186/s12934-017-0793-7.
62. Schindelin J, Arganda-Carreras I, Frise E, Kaynig V, Longair M, Pietzsch T, Preibisch S, Rueden C, Saalfeld S, Schmid B, Tinevez J-Y, White DJ, Hartenstein V, Eliceiri K, Tomancak P, Cardona A. 2012. Fiji: an open-source platform for biological-image analysis. Nat Methods 9:676–682. https://doi.org/10.1038/nmeth.2019.
63. Karasov TL, Almario J, Friedemann C, Ding W, Giolai M, Heavens D, Kersten S, Lundberg DS, Neumann M, Regalado J, Neher RA, Kemen E, Weigel D. 2018. Arabidopsis thaliana and Pseudomonas pathogens exhibit stable associations over evolutionary timescales. Cell Host Microbe 24:168–179.e4. https://doi.org/10.1016/j.chom.2018.06.011.
64. Droop AP. 2016. fqtools: an efficient software suite for modern FASTQ file manipulation. Bioinformatics 32:1883–1884. https://doi.org/10.1093/bioinformatics/btw088.
65. Jiang H, Lei R, Ding S-W, Zhu S. 2014. Skewer: a fast and accurate adapter trimmer for next-generation sequencing paired-end reads. BMC Bioinformatics 15:182. https://doi.org/10.1186/1471-2105-15-182.
66. Ewels P, Magnusson M, Lundin S, Käller M. 2016. MultiQC: summarize analysis results for multiple tools and samples in a single report. Bioinformatics 32:3047–3048. https://doi.org/10.1093/bioinformatics/btw354.
67. Garcia-Betancur JC, Yepes A, Schneider J, Lopez D. 2012. Single-cell analysis of Bacillus subtilis biofilms using fluorescence microscopy and flow cytometry. J Vis Exp 2012:3796. https://doi.org/10.3791/3796.
68. Zhang H, DiBaise JK, Zuccolo A, Kudrna D, Braidotti M, Yu Y, Parameswaran P, Crowell MD, Wing R, Rittmann BE, Krajmalnik-Brown R. 2009. Human gut microbiota in obesity and after gastric bypass. Proc Natl Acad Sci U S A 106:2365–2370. https://doi.org/10.1073/pnas.0812600106.
69. Turnbaugh PJ, Hamady M, Yatsunenko T, Cantarel BL, Duncan A, Ley RE, Sogin ML, Jones WJ, Roe BA, Affourtit JP, Egholm M, Henrissat B, Heath AC, Knight R, Gordon JI. 2009. A core gut microbiome in obese and lean twins. Nature 457:480–484. https://doi.org/10.1038/nature07540.